Materials Transactions, Vol. 43, No. 11 (2002) pp. 2843 to 2846

Formation, Thermal Stability and Mechanical Properties in Zr–Al–Co Bulk Glassy Alloys

Takeshi Wada[1, *], Tao Zhang[2] and Akihisa Inoue[2]

[1]*Graduate School, Tohoku University, Sendai 980-8579, Japan*
[2]*Institute for Materials Research, Tohoku University, Sendai 980-8577, Japan*

A Zr–Al–Co ternary alloy was investigated in order to clarify the glass-forming ability, thermal stability and mechanical properties. The $Zr_{55}Al_{20}Co_{25}$ alloy was found to be fabricated in bulk glassy alloy rods with diameters up to at least 2.5 mm. The glassy alloy rod of 2.5 mm in diameter exhibits a large supercooled liquid region of 79 K, followed by a nearly single exothermic peak due to the precipitation of ZrCo + ZrAlCo + Zr_6Al_2Co phases. The glassy alloy rod exhibits Young's modulus of 114 GPa, high compressive fracture strength of 1900 MPa and total fracture elongation of 1.7%. The finding of forming the bulk glassy alloy at the new ternary composition of $Zr_{55}Al_{20}Co_{25}$ by the copper mold casting method is encouraging for future search of a new glassy alloy composition.

(Received May 15, 2002; Accepted September 17, 2002)

Keywords: *bulk glassy alloy, zirconium–aluminum–cobalt system, casting, supercooled liquid, high mechanical strength*

1. Introduction

It is well known that bulk glassy alloys have been produced in a number of alloy systems such as lanthanide (Ln)-,[1)] Mg-,[2)] Zr-,[3,4)] Ti-,[5)] Fe-,[6)] Pd–Cu-,[7)] Co-,[8)] Ni-,[9)] Cu-[10)] and Ca-[11)] bases for the last one and a half decades. Among these bulk glassy alloy systems, the Zr- and Cu-based alloys exhibit high mechanical strength combined with high ductility and hence have attracted great interest as a new type of bulk structural materials. When we pay attention to Zr-based bulk glassy alloys, the alloy systems can be classified into two groups, *i.e.*, Zr–Al–Ni–Cu[12)] and Zr–Al–Ni–Cu–(Ti, Nb, Pd)[13,14)] systems developed by Sendai group and Zr–Ti–Ni–Cu–Be[4)] system developed by Caltech group. Very recently, Sendai group has succeeded in developing the third type of Zr-based bulk glassy alloy system as presented by Zr–Al–Co and Zr–Al–Fe base systems.[15)] The new Zr-based alloys have some features of higher Al contents of 10 to 25 at% and higher mechanical strength of 1800 to 1900 MPa which cannot be obtained for the previously reported two kinds of Zr-based bulk glassy alloys. In addition, when the application of Zr-based bulk glassy alloys to biomedical materials is taken into consideration, it is important to develop a new Zr-based bulk glassy alloy without any toxic elements such as Ni and Be. In the previous paper, we have reported that bulk glassy alloy rods in the diameter range up to 5 mm are formed for $Zr_{55}Al_{20}Co_{20}Cu_5$ and the tensile fracture strength reaches 1960 MPa.[15)] However, little is known about thermal stability of supercooled liquid, solidification behavior and mechanical properties for the new Zr–Al–Co ternary alloys. This information is essential for the evaluation of bulk glass-forming ability as well as for the determination of a more appropriate production method. This paper intends to present the thermal stability of the supercooled liquid including the liquidus temperatures in Zr–Al–Co system and to investigate an optimum alloy composition at which the highest glass-forming ability combined with high mechanical strength is obtained.

2. Experimental Procedure

Ternary alloy ingots with composition of $Zr_{100-x-y}Al_xCo_y$ were prepared by arc melting the mixture of pure Zr, Al and Co metals in an argon atmosphere. The alloy composition represents nominal atomic percentages. Alloy rods with different diameters up to 5 mm were prepared by the copper mold casting method. Alloy ribbons with a cross section of $0.02 \times 1.2\,mm^2$ were also prepared for comparison by the melt spinning technique. The glassy structure was examined by X-ray diffraction (XRD) and optical microscopy (OM). Thermal stability associated with glass transition, supercooled liquid region and crystallization temperature was examined by differential scanning calorimetry (DSC) at a heating rate of 0.67 K/s. Liquidus temperatures were also measured by differential thermal analysis (DTA) at a low cooling rate of 0.067 K/s. Reduced glass transition temperature was calculated to evaluate the thermal stability of glassy phase. Mechanical properties were measured with an Instron testing machine. The gauge dimension of the testing specimens was 2.5 mm in diameter and 5 mm in height for the compressive deformation mode and the strain rate was $5 \times 10^{-4}\,s^{-1}$. The fracture surface was examined by scanning electron microscopy (SEM).

3. Results

Figure 1 shows the DSC curves of the melt-spun $Zr_{55}Al_xCo_{45-x}$ (x = 12, 16, 20, 24 and 28 at%) glassy alloy ribbons. All the alloys exhibit the sequent transition of glass transition, followed by supercooled liquid region and then crystallization. The glass transition temperature (T_g) remains almost unchanged in the Al content range of 12 to 24 at%, but the crystallization temperature (T_x) increases and shows a maximum value of 838 K for the 20 at%Al alloy, accompanying the change from the distinctly separated two exothermic peaks to a nearly single exothermic peak. With further increasing Al content, the crystallization mode changed again

*Graduate Student, Tohoku University.

to two-stage exothermic reactions.

The similar DSC curves were also obtained for the other alloy series of $Zr_{50}Al_xCo_{50-x}$ and $Zr_{60}Al_xCo_{40-x}$. Based on the data of these DSC curves, the composition dependence of $\Delta T_x (= T_x - T_g)$ is shown in Fig. 2. The ΔT_x value has a distinct composition dependence. That is, the largest ΔT_x of 79 K is obtained for $Zr_{55}Al_{20}Co_{25}$ and decreases significantly with a deviation of alloy composition from $Zr_{55}Al_{20}Co_{25}$. The large composition dependence of ΔT_x is consistent with the previous data[12–14] in which no large supercooled liquid region was obtained for $Zr_{60}Al_{10}Co_{30}$ alloy, though the $Zr_{60}Al_{10}Ni_{30}$ and $Zr_{60}Al_{10}Cu_{30}$ glassy alloys exhibit a large supercooled liquid region above 50 K.[3,12]

Figure 3 shows an XRD pattern of the melt-spun $Zr_{55}Al_{20}Co_{25}$ ribbon annealed at 950 K for 600 s. One can see a number of sharp diffraction peaks indicating the presence of crystalline phases. These phases are identified as a mixed structure of ZrCo, ZrAlCo and Zr_6Al_2Co, as analyzed in the Fig. 3.

Figure 4 shows the DTA curves of the alloy series $Zr_{55}Al_xCo_{45-x}$. It is seen that the onset temperature of the exothermic peak marked with T_l decreases significantly with increasing Al content up to 20 at% and then increases with further increasing Al content, leading to a minimum T_l value for $Zr_{55}Al_{20}Co_{25}$. Figure 5 shows the composition depen-

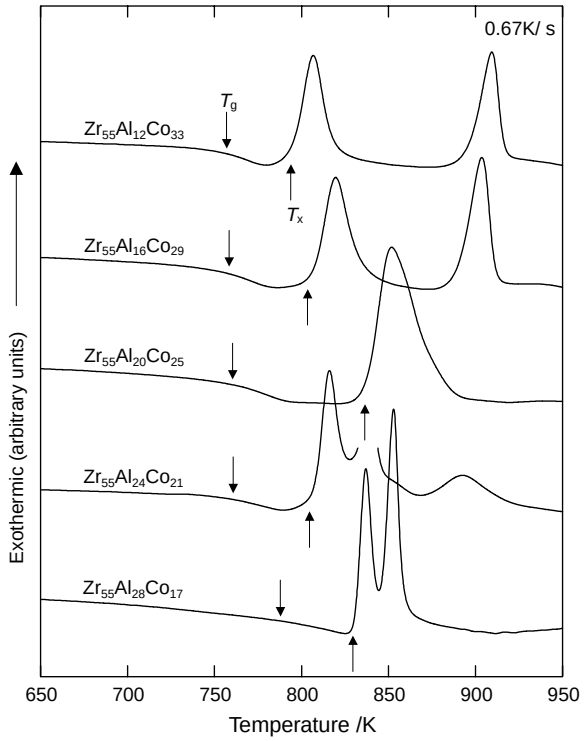

Fig. 1 DSC curves of melt-spun $Zr_{55}Al_xCo_{45-x}$ (x = 12, 16, 20, 24 and 28 at%) glassy alloys.

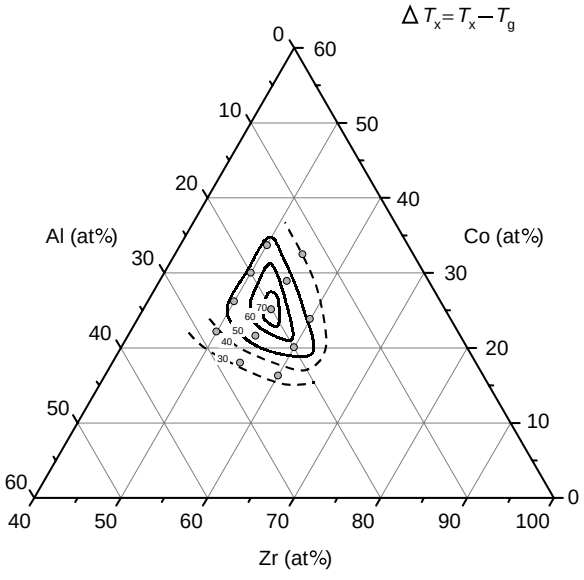

Fig. 2 Composition dependence of supercooled liquid region $\Delta T_x (= T_x - T_g)$ of melt-spun Zr–Al–Co glassy alloys.

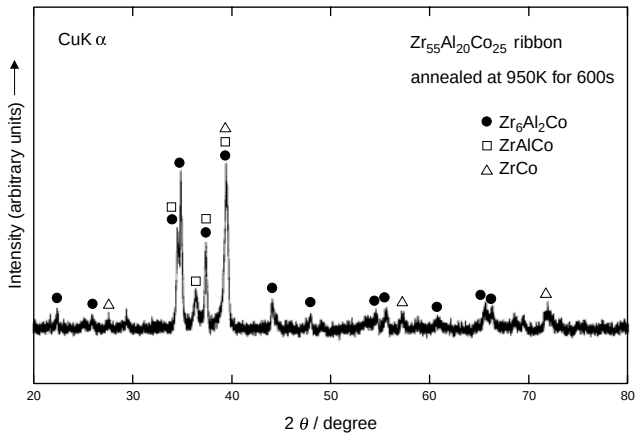

Fig. 3 XRD pattern of a melt-spun $Zr_{55}Al_{20}Co_{25}$ alloy ribbon annealed at 950 K for 600 s.

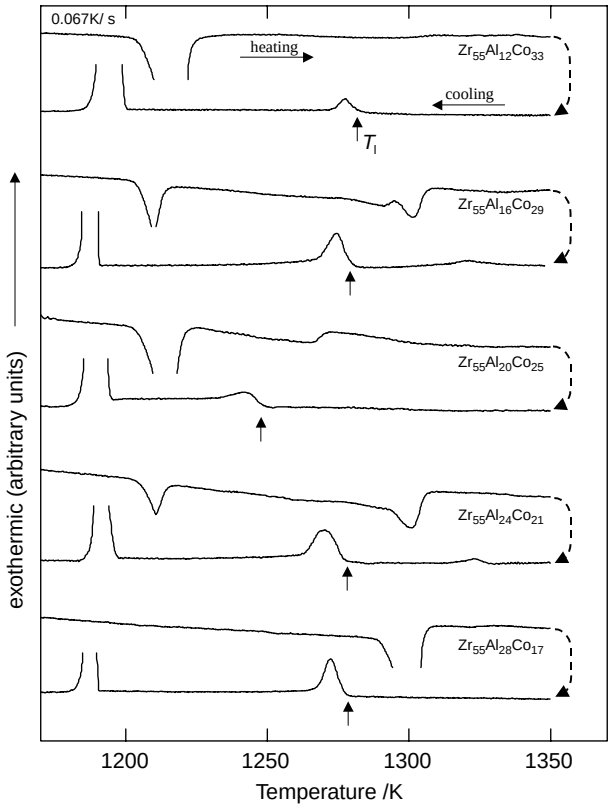

Fig. 4 DTA curves of $Zr_{55}Al_xCo_{45-x}$ (x = 12 to 28 at%) alloys.

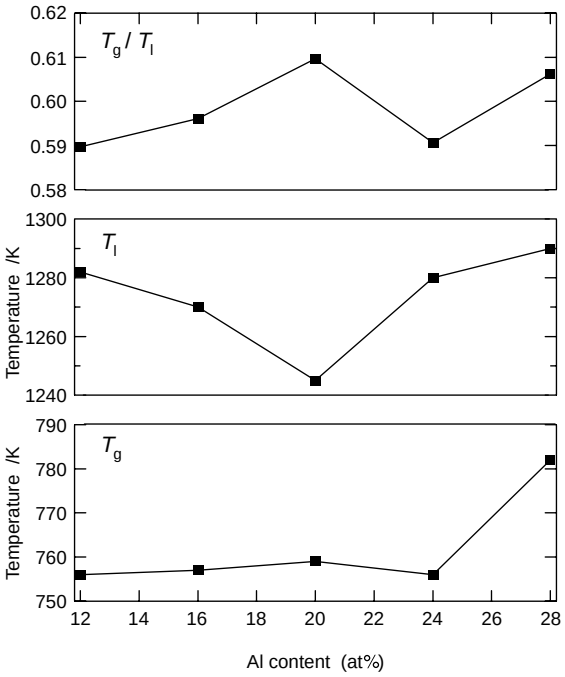

Fig. 5 Composition dependence of T_g, T_l, and T_g/T_l for the glassy $Zr_{55}Al_xCo_{45-x}$ alloys.

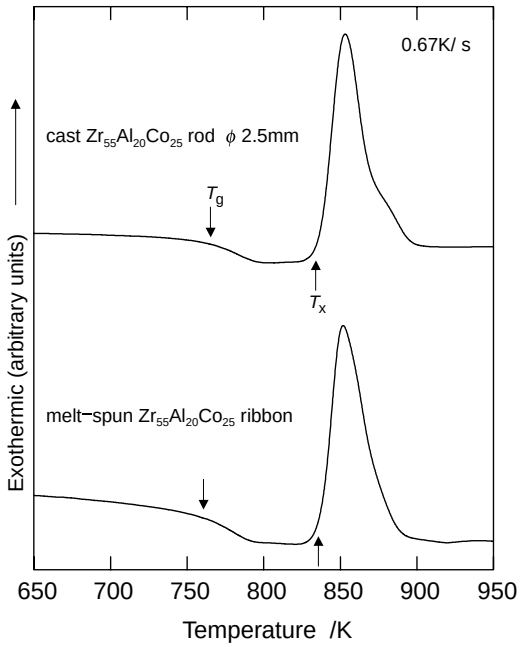

Fig. 6 DSC curve of a cast $Zr_{55}Al_{20}Co_{25}$ glassy alloy rod with a diameter of 2.5 mm. The data of the melt-spun Zr–Al–Co glassy alloy ribbon are also shown for comparison.

dence of T_g, T_l and reduced glass transition temperature (T_g/T_l) for the $Zr_{55}Al_xCo_{45-x}$ glassy alloys. The highest T_g/T_l of 0.61 is obtained for $Zr_{55}Al_{20}Co_{25}$ alloy. Considering the general tendency for glass-forming ability to increase with increasing T_g/T_l which has been recognized for a number of glassy alloys,[17] it is expected that the highest glass-forming ability is obtained at this composition. In addition, bulk glassy alloys have usually been obtained for the alloys with T_g/T_l above 0.60[17] and hence the $Zr_{55}Al_{20}Co_{25}$ alloy seems to have a bulk glass-forming ability which enables the formation of a bulk glassy alloy by casting processes. The close correlation between glass-forming ability and T_g/T_l has been interpreted to result from higher stability of liquid phase for the alloys with lower T_l and high viscosity for the alloys with high T_g.

We examined the bulk glass-forming ability of the $Zr_{55}Al_{20}Co_{25}$ alloy by the copper mold casting method. It was confirmed that a glassy single phase is formed in the diameter range up to at least 2.5 mm. Figure 6 shows the DSC curve of the cast $Zr_{55}Al_{20}Co_{25}$ glassy alloy rod with a diameter of 2.5 mm, together with the data of the corresponding melt-spun glassy ribbon. No distinct difference in the T_g, ΔT_x, T_x and crystallization-induced exothermic peak derived from the DSC curves is seen in the rod and ribbon samples, indicating the formation of a similar glassy structure for both samples. The alloy rod of 2.5 mm in diameter exhibited high compressive fracture strength ($\sigma_{c,f}$) of 1900 MPa and Young's modulus (E) of 114 GPa, accompanying the total fracture elongation of 1.7% including elastic elongation of 1.5%. It is noticed that the ($\sigma_{c,f}$) is higher than that (1500–1700 MPa)[12–14] of previously reported Zr-based bulk glassy alloys. The fracture mode as well as the fracture surface structure agrees well with that for other Zr-based bulk glassy alloys in Zr–Al–Ni–Cu system.[18]

4. Discussion

It was shown that the glassy alloy composition with the largest ΔT_x is located in the vicinity of $Zr_{55}Al_{20}Co_{25}$. It is characterized that the Al content is about two times higher than the optimum Al content (about 10 at%)[16,17] of Zr–Al–Ni and Zr–Al–Cu ternary bulk glassy alloys. Here, we discuss the reason for the significant difference in the optimum Al contents for bulk glass formation. One can notice some significant differences in the equilibrium phase diagrams between Co–Al and Ni–Al or Cu–Al binary systems. That is, the Co-, Ni- and Cu-rich intermetallic compounds in an equilibrium state are CoAl, Ni_3Al and Cu_3Al phases, respectively.[19] Thus, there is no Co_3Al-type equilibrium compound with a low Al content of 25 at%. The necessity of the much higher Al content for formation of the stable compound implies that the bonding force of Co–Al pair may be considerably weaker than those for Ni–Al and Cu–Al pairs. The difficulty of forming the intermetallic compound in the lower Al content range around 25 at%Al in Co–Al system may be the reason why the bonding state required for formation of the more stable glassy structure is attained by the dissolution of the much larger amount of Al content. A more detailed study on the atomic configurations around Al element will shed light on the reason for significant difference in the optimum Al content for formation of the bulk glassy alloys among Zr–Al–M (M=Co, Ni and Cu) alloys.

5. Summary

We examined the stability of supercooled liquid against crystallization for the alloy series of $Zr_{60}Al_xCo_{40-x}$, $Zr_{55}Al_xCo_{45-x}$ and $Zr_{50}Al_xCo_{50-x}$, with the aim of determining an appropriate composition for formation of a bulk glassy alloy in Zr–Al–Co ternary system. The results obtained are

summarized as follows;

(1) The largest supercooled liquid region defined by the difference between T_g and T_x, $\Delta T_x (= T_x - T_g)$ was 79 K for $Zr_{55}Al_{20}Co_{25}$ and decreased significantly with deviation of alloy composition.

(2) The glassy alloy crystallizes through a nearly single exothermic peak due to the precipitation of ZrCo + ZrAlCo + Zr_6Al_2Co phases.

(3) The largest reduced glass transition temperature defined by T_g/T_l is 0.61 for $Zr_{55}Al_{20}Co_{25}$ alloy.

(4) The use of the $Zr_{55}Al_{20}Co_{25}$ alloy enabled us to form bulk glassy alloy rods with diameters up to 2.5 mm and the glassy rod of 2.5 mm in diameter exhibits compressive fracture strength of 1900 MPa combined with total fracture elongation of 1.7%.

The formation of the bulk glassy alloy in the simple Zr–Al–Co ternary system provides basic information for future extension to more multi-component systems in which a bulk glassy alloy with much larger maximum sample diameter can be formed by the conventional casting method.

REFERENCES

1) A. Inoue, T. Zhang and T. Masumoto: Mater. Trans., JIM **30** (1989) 965–972.
2) A. Inoue, K. Ohtera, K. Kita and T. Masumoto: Jpn. J. Appl. Phys. **27** (1989) L2258–L2261.
3) A. Inoue, T. Zhang and T. Masumoto: Mater. Trans., JIM **31** (1990) 177–183.
4) A. Pecker and W. L. Johnson: Appl. Phys. Lett. **63** (1993) 2342–2344.
5) A. Inoue, T. Zhang, N. Nishiyama, K. Ohba and T. Masumoto: Mater. Lett. **19** (1994) 131–135.
6) A. Inoue and G. S. Gook: Mater. Trans., JIM **36** (1995) 1180–1183.
7) A. Inoue, N. Nishiyama and T. Matsuda: Mater. Trans., JIM **37** (1996) 181–184.
8) T. Itoi and A. Inoue: Mater. Trans., JIM **41** (2000) 1256–1262.
9) X. Wang, I. Yoshii and A. Inoue: Mater. Trans., JIM **41** (2000) 539–542.
10) A. Inoue, W. Zhang, T. Zhang and K. Kurosaka: Acta Mater. **49** (2001) 2645–2652.
11) K. Amiya and A. Inoue: Mater. Trans. **43** (2002) 81–84.
12) T. Zhang, A. Inoue and T. Masumoto: Mater. Trans., JIM **32** (1991) 1005–1010.
13) A. Inoue, T. Shibata and T. Zhang: Mater. Trans., JIM **36** (1995) 1420–1426.
14) A. Inoue, Y. Yokoyama, Y. Shinohara and T. Masumoto: Mater. Trans., JIM **35** (1994) 923–926.
15) T. Zhang and A. Inoue: Mater. Trans. **43** (2002) 1250–1253.
16) A. Inoue: Mater. Trans., JIM **36** (1995) 866–875.
17) A. Inoue: Acta Mater. **48** (2000) 279–306.
18) A. Inoue: *Bulk Amorphous Alloys, Practical Characteristics and Applications*, (Trans Tech Publications, Zurich, 1999) pp. 2–6.
19) *Binary Alloy Phase Diagrams*, ed. by T. B. Massalski (ASM International, Materials Park, Ohio, 1990).